

DETC2015-47266

## SELF-EXCITED LATERAL VIBRATIONS OF ROLLING TIRES

**Dénes Takács**

MTA-BME Research Group on Dynamics  
of Machines and Vehicles  
Budapest, Hungary  
Email: takacs@mm.bme.hu

**Gábor Stépan**

Department of Applied Mechanics  
Budapest University of Technology and Economics  
Budapest, H-1521, Hungary  
Email: stepan@mm.bme.hu

### ABSTRACT

*In this study, a low degree-of-freedom mechanical model of a rolling tire is constructed, in which the lateral deformation of the contact patch and tire carcass is considered. The so-called delayed contact patch model is implemented and combined with a simple tire carcass model. The interaction between the contact patch and the carcass together with the lateral mode of the attached suspension system is modeled by means of minimum number of relevant parameters in a simplified way in order to construct analytical results. Critical parameter ranges of self-excited vibrations are determined against the longitudinal speed of the tire. The intricate shapes of the corresponding tire deformations are presented by means of numerical simulations.*

### NOMENCLATURE

- $a$  Half length of the contact patch.
- $m$  Mass of the wheel.
- $k$  Specific stiffness of the tire.
- $k_s$  Lateral stiffness of the suspension.
- $q$  Lateral deformation of the tire in the contact patch.
- $R$  Radius of the undeformed tire.
- $t$  Time.
- $v$  Longitudinal speed of the center point of the wheel.
- $w$  Lateral deformation outside the contact patch.
- $Y_C$  Lateral displacement of the center point of the wheel.
- $\omega_c$  Natural angular frequency of a tire brush element.
- $\rho A$  Distributed mass of the tire.
- $\tau_1$  Time delay in the contact patch.

$\tau_2$  Time delay outside the contact patch.

### INTRODUCTION

The shimmy of motorcycles [1, 2], steered wheels of cars and the airplane gears [3–5] is a well known phenomenon in vehicle dynamics. Although this phenomenon dates back to the appearance of the first vehicles [6], it requires special attention of engineers in the design stage even nowadays. The safety hazard of shimmy induced many publications about the lateral vibration of towed wheels. Moreover, the investigation of shimmy leads to improved and detailed models of tires and tire/road interactions.

It was recognized very early that the tire/ground contact patch is responsible for a kind of memory effect [7], but the available mathematical theories and methods did not allow engineers at that time to analyze delay differential equations, while an engineering approximation of the tire lateral deformation in the contact patch helped to explore some properties of the shimmying tire [8, 9]. Later, the accurate modeling of the contact patch lateral deformation and the analysis of the corresponding delay differential equations provided new explanations for some quasi-periodic vibrations [10] and also uncovered new parameter domains where so-called micro-shimmy exists [11]. The application of this time delayed contact patch description in the single track car model [12] and in the single track car-trailer model [13] also identified parameter ranges where small amplitude lateral vibrations may appear. These vibrations can be neglected in view of the lateral stability of the vehicles but they are relevant components in the noise generation.

Noise generation of tires has become an important aspect of tire design in recent decades. There are several studies (see, for example, [14–17]) in this field, which include detailed tire/ground contact patch and tire carcass models but do not consider the dynamics of the attached vehicle system. This is due to the fact that the major part of the noise of tires is originated in the so-called horn effect, which does not have any relation to the tire attached suspension system.

Here, we present a simple mechanical model of a brush tire model that is supported by a laterally elastic suspension. This mechanical mode is a special case of classical shimmy models in case of infinite caster length, that is, the wheel cannot rotate about the vertical axis. Namely, a lateral mode of the attached suspension-wheel system is considered, in which the delayed contact patch model is combined with a tire carcass model. Critical parameter ranges of self-excited vibrations are determined versus the longitudinal speed of the tire with special attention to the frequencies of these vibrations. Some numerical simulation are presented to illustrate the traveling deformation waves along the tire circumference both in the contact patch and outside the contact patch.

## MECHANICAL MODEL

The mechanical model in question is shown in Fig. 1. The wheel of elastic tire is rolling in the ground-fixed  $(X, Y, Z)$  coordinate system; its longitudinal speed  $v$  is kept constant. The rotational axis of the wheel of tire is supported in lateral direction by the spring of stiffness  $k_s$ . The lateral position of the wheel center point is described by  $Y_C(t)$  as a function of the time  $t$ . The mass of the wheel is denoted by  $m$ . The  $(x, y, z)$  coordinate system is fixed to the wheel center point, its axes are parallel to the axes of the  $(X, Y, Z)$  coordinate system.

The radius of the undeformed tire is  $R$ . The tire is in contact with the ground along the contact patch of length  $2a$ . The deformation in the longitudinal dimension of the tire is neglected in this study, while the lateral tire deformation is described by  $q(x, t)$  in the contact patch and by  $w(\chi, t)$  outside the contact patch. As it is shown in Fig. 1, the angle  $\chi \in [0, \beta]$  (where  $\beta = 2(\pi - \alpha)$  and  $\alpha = \arcsin(a/R)$ ) sweeps along the circumference of the tire starting from the trailing edge R ending at the leading edge L of the contact patch.

In this study, we use the so-called brush tire model, which considers separated tire particles along the circumference of the tire. These tire particles are viewed like the thread elements of the tire, namely, their lateral deformations are independent. The distributed mass of the tire particles is characterized by  $\rho A$  [kg/m], and the specific lateral stiffness  $k$  [N/m<sup>2</sup>] relates to the distributed elastic support of the tire particles.

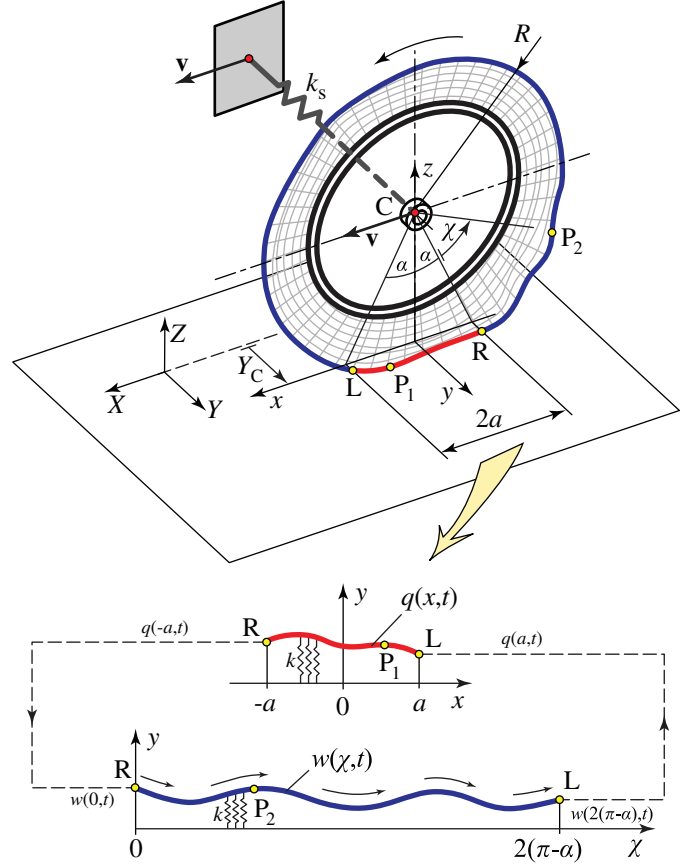


FIGURE 1. THE MECHANICAL MODEL.

### Tire deformation in the contact patch

In the contact patch, we consider pure rolling, namely, the tire particles attached to the ground have zero velocities. The position vector of a tire particle  $P_1$  can be given in the  $(X, Y, Z)$  coordinate system as

$$\mathbf{R}_{P_1} = \begin{bmatrix} vt + x \\ Y_C(t) + q(x, t) \\ 0 \end{bmatrix}, \quad (1)$$

for  $x \in [-a, a]$ . The velocity is

$$\frac{d}{dt} \mathbf{R}_{P_1} = \begin{bmatrix} v + \dot{x} \\ \dot{Y}_C(t) + \dot{q}(x, t) + q'(x, t)\dot{x} \\ 0 \end{bmatrix}. \quad (2)$$

Here, dot and prime refer to the partial derivatives with respect to time and space coordinates, respectively. As it was mentioned, the kinematic constraint of rolling means that  $\frac{d}{dt} \mathbf{R}_{P_1} = \mathbf{0}$ . Substituting the first row of this equation into the second one, we obtain

the partial differential equation (PDE):

$$\dot{q}(x, t) = -\dot{Y}_C(t) + q'(x, t)v \quad (3)$$

for  $x \in [-a, a]$ .

### Tire deformation outside the contact patch

The equations of motion of the tire particles outside the contact patch were derived with the combination of both Newton's Laws and Hamilton's Principle. The standard form of Hamilton's Principle is only partially applicable for moving continua because of the material transfer at the boundaries, which can increase and dissipate the energy of the system. Accordingly, Hamilton's Principle has to be extended by a term (see [18]), which describes the variation of the material flow at the boundaries. In case of prismatic continua this term vanishes in some special cases, for example, when fixed supports are located at the boundaries (see [19]). In our case, the deformations are free at the points R and L although the absolute velocities of the tire particles are zeros at these points since we consider rolling. Due to the fact that the lateral deformations of the separated brush elements are independent, the standard form of Hamilton's Principle can be used. The Lagrangian can be given as the difference of the kinetic energy and the potential function of the spring forces:

$$L = \frac{1}{2} \int_0^\beta (\rho A \mathbf{v}_{P_2}^2(\chi, t) - k w^2(\chi, t)) R d\chi, \quad (4)$$

where  $\mathbf{v}_{P_2}(\chi, t)$  refers to the velocity of the tire particle at the position  $\chi$ :

$$\mathbf{v}_{P_2}(\chi, t) = \begin{bmatrix} v(1 - \cos(\alpha + \chi)) \\ \dot{Y}_C(t) + \dot{w}(\chi, t) + \frac{v}{R} w'(\chi, t) \\ v \sin(\alpha + \chi) \end{bmatrix}. \quad (5)$$

The translational rate of change of the tire particles is assumed to be equal to the longitudinal speed  $v$  of the wheel center point.

According to Hamilton's Principle, the functional

$$I = \int_{t_1}^{t_0} L dt \quad (6)$$

is extremal at the real motion of the tire particles, i.e.  $\delta I = 0$ . This condition can be formulated by means of the Euler-Lagrange equation, which formulates the variational problem as differential equations. Considering Eqn. (5) in Eqn. (4), Eqn. (6) can be composed in the form of

$$I = \int_{t_0}^{t_1} \int_0^\beta F(w, \dot{w}, w', \chi, t) d\chi dt. \quad (7)$$

Thus, the Euler-Lagrange equation leads to

$$\frac{dF}{dw} - \frac{\partial}{\partial t} \frac{\partial F}{\partial \dot{w}} - \frac{\partial}{\partial \chi} \frac{\partial F}{\partial w'} = 0. \quad (8)$$

Thus, the tire deformation is characterized by the partial differential equation:

$$\ddot{w}(\chi, t) + \frac{2v}{R} \dot{w}'(\chi, t) + \frac{v^2}{R^2} w''(\chi, t) + \omega_c^2 w(\chi, t) + \dot{Y}_C(t) = 0, \quad (9)$$

for  $\chi \in [0, \beta]$ . In the equation

$$\omega_c = \sqrt{\frac{k}{\rho A}} \quad (10)$$

refers to the natural angular frequency of the lateral vibrations of the tire brush element.

### Equation of motion

The equation of motion of the wheel, which is attached to the laterally elastic suspension, can easily be derived with the help of Newton's Law. Here we present the equation without detailed explanations:

$$m \ddot{Y}_C(t) + k_s Y_C(t) = k \int_{-a}^a q(x, t) dx + k \int_0^\beta w(\chi, t) R d\chi. \quad (11)$$

This equation is coupled to Eqn. (3) and Eqn. (9). The boundary conditions (BCs) of the PDEs are:

$$\begin{aligned} q(a, t) &= w(\beta, t), \\ w(0, t) &= q(-a, t), \\ w'(0, t) &= -R q'(-a, t). \end{aligned} \quad (12)$$

The first two BCs correspond to the continuity of the lateral deformation at the leading edge L and at the trailing edge R, respectively. The third one (no kink at R) is based on  $\frac{d}{dt} w(0, t) = \frac{d}{dt} q(-a, t)$ , which describes the initial lateral speed of the deformation waves that propagate along the circumference of the tire outside the contact patch.

### TIME DELAYED TIRE MODEL

#### The contact patch memory

The memory effect of the tire/ground contact patch is known since von Schlippe already identified this property of tires in [7].

In case of rolling the tire particles stick to the ground and keep their positions during the contact. Consequently, their positions at the time instant  $t$  were determined when they reached the ground at the leading edge at  $t - \tau_1(x)$ . The time delay  $\tau_1(x)$  characterizes the time interval, which was needed for a tire particle to travel backwards in the contact patch from the leading edge L to its actual position  $x$  (see Fig. 1). Thus, the traveling wave solution of the PDE in Eqn. (3) can be determined in the form:

$$q(x, t) = -Y_C(t) + Y_C(t - \tau_1(x)) + q(a, t - \tau_1(x)) \quad (13)$$

for  $x \in [-a, a]$ . The time delay has a physically obvious form:

$$\tau_1(x) = \frac{a - x}{v}. \quad (14)$$

### Traveling wave solution outside the contact patch

Since the tire particles travels with constant translational speed along the circumference of the tire, a traveling wave solution can also be composed for Eqn. (9). Based on the Duhamel's integral formula:

$$\begin{aligned} w(\chi, t) &= w(0, t - \tau_2(\chi)) \cos(\omega_c \tau_2(\chi)) \\ &+ \frac{1}{\omega_c} \frac{d}{dt} w(0, t - \tau_2(\chi)) \sin(\omega_c \tau_2(\chi)) \\ &- \frac{1}{\omega_c} \int_0^{\tau_2(\chi)} \ddot{Y}_C(t - \tau_2(\chi) + \vartheta) \sin(\omega_c(\tau_2(\chi) - \vartheta)) d\vartheta, \end{aligned} \quad (15)$$

where the time delay:

$$\tau_2(\chi) = \frac{R\chi}{v}. \quad (16)$$

### Closed loop of traveling waves

Using the second and the third BCs of Eqn. (12), the traveling wave solution Eqn. (15) can be composed as a function of the trailing edge deformation of the contact patch:

$$\begin{aligned} w(\chi, t) &= q(-a, t - \tau_2(\chi)) \cos(\omega_c \tau_2(\chi)) \\ &+ \frac{1}{\omega_c} \frac{d}{dt} q(-a, t - \tau_2(\chi)) \sin(\omega_c \tau_2(\chi)) \\ &- \frac{1}{\omega_c} \int_0^{\tau_2(\chi)} \ddot{Y}_C(t - \tau_2(\chi) + \vartheta) \sin(\omega_c(\tau_2(\chi) - \vartheta)) d\vartheta. \end{aligned} \quad (17)$$

Using the traveling wave solution Eqn. (13), the trailing edge deformation can be given as

$$\begin{aligned} q(-a, t - \tau_2(\chi)) &= -Y_C(t - \tau_2(\chi)) + Y_C(t - \tau_2(\chi) - T_1) \\ &+ q(a, t - \tau_2(\chi) - T_1), \end{aligned} \quad (18)$$

where

$$T_1 = \tau_1(-a) \equiv \frac{2a}{v} \quad (19)$$

refers to the time interval that is needed for a tire particle to travel along the contact patch.

After the substitution of Eqn. (18) into Eqn. (17), the first BC of Eqn. (12) leads to:

$$\begin{aligned} q(a, t) &= (-Y_C(t - T_2) + Y_C(t - T_1 - T_2)) \cos(\omega_c T_2) \\ &+ q(a, t - T_1 - T_2) \cos(\omega_c T_2) - \frac{1}{\omega_c} \dot{Y}_C(t - T_2) \sin(\omega_c T_2) \\ &- \frac{1}{\omega_c} \int_0^{T_2} \ddot{Y}_C(t - T_2 + \vartheta) \sin(\omega_c(T_2 - \vartheta)) d\vartheta, \end{aligned} \quad (20)$$

where

$$T_2 = \tau_2(\beta) \equiv \frac{R\beta}{v} \equiv \frac{2R(\pi - \alpha)}{v} \quad (21)$$

is the time interval, which is needed for a tire particle to travel along the circumference of the tire from the trailing edge R to the leading edge L.

Using Eqns. (13) and (17) with Eqn. (18) in Eqn. (11), one can eliminate the deformation functions  $q(x, t)$  and  $w(\chi, t)$  and the corresponding PDEs given in Eqns. (3) and (9). Thus, the governing equations of the system reduce to:

$$\begin{aligned} m\ddot{Y}_C(t) + k_s Y_C(t) &= -kv \int_0^{T_1} Y_C(t) - Y_C(t - \tau_1) - q(a, t - \tau_1) d\tau_1 \\ &- kv \int_0^{T_2} (Y_C(t - \tau_2) - Y_C(t - \tau_2 - T_1)) \cos(\omega_c \tau_2) d\tau_2 \\ &+ kv \int_0^{T_2} q(a, t - \tau_2 - T_1) \cos(\omega_c \tau_2) d\tau_2 \\ &- \frac{kv}{\omega_c} \int_0^{T_2} \dot{Y}_C(t - \tau_2) \sin(\omega_c \tau_2) d\tau_2 \\ &- \frac{kv}{\omega_c} \int_0^{T_2} \int_0^{\tau_2} \ddot{Y}_C(t - \tau_2 + \vartheta) \sin(\omega_c(\tau_2 - \vartheta)) d\vartheta d\tau_2, \end{aligned} \quad (22)$$

which is coupled to Eqn. (20). It can be seen that the substitution of  $q(a, t)$  leads to a neutral type distributed delay differential equation.

## STABILITY ANALYSIS

### Tire with rigid suspension

In order to illustrate the interaction of the deformations of the contact patch and the non-contacting part of the tire, a further simplification of our mechanical model is used in this section. Consider a perfectly rigid suspension system in the mechanical model, i.e.  $k_s \rightarrow \infty$ , which means that lateral displacement of the wheel center point is blocked. In this case  $Y_C(t) \equiv 0$  and the equation of motion Eqn. (11) can be omitted. Moreover, the traveling wave solutions Eqns. (13) and (15) simplify, consequently, Eqn. (20) reduces to

$$q(a, t) = \cos(\omega_c T_2) q(a, t - T_1 - T_2). \quad (23)$$

This scalar difference equation governs the system in case of the rigid suspension. The stability of the system depends on the coefficient  $\cos(\omega_c T_2)$ . If  $|\cos(\omega_c T_2)| < 1$  then the system is asymptotically stable and the vibrations of the tire particles decay in time. The limit of stability corresponds to  $|\cos(\omega_c T_2)| = 1$ , which gives the critical longitudinal speeds

$$v_{cr,j} = \frac{2R\omega_c(1 - \alpha/\pi)}{j} \quad j = 0, 1, 2, \dots \quad (24)$$

For these speeds, the lateral vibrations of the tire particles do not decay in time. On the contrary, the fastest decay relates to  $\cos(\omega_c T_2) = 0$ , which leads to

$$v_{fav,j} = \frac{2R\omega_c(1 - \alpha/\pi)}{j + 1/2} \quad j = 0, 1, 2, \dots \quad (25)$$

In case of  $v = v_{fav,j}$ , the vibration of the tire particles are fully dissipated by the contact patch within one rotation of the wheel.

### Tire with elastic suspension

Let consider our original system, which is governed by Eqns. (20) and (22). One can substitute the exponential trial solutions  $Y_C(t) = Y e^{\lambda t}$  and  $q(a, t) = Q e^{\lambda t}$  into these equations and can calculate the characteristic function  $D(\lambda)$  of the system. Here we do not present the formula of the characteristic function.

One can determine that  $\lim_{\lambda \rightarrow 0} D(\lambda) = 0$  is satisfied for the critical speeds of Eqn. (24). This suggests that some properties of this model are inherited by the properties of the simpler, rigid

**TABLE 1.** THE PARAMETERS OF THE CASE STUDY.

Parameter	Value
$a$	0.04 m
$R$	0.2 m
$k$	60 kN/m <sup>2</sup>
$\rho A$	0.4 kg/m
$k_s$	1 kN/m
$m$	2 kg

suspension model. But in case of elastic suspension, the system presents a much richer dynamics, of course.

According to the D-subdivision method, the stability boundaries can be determined if we substitute  $\lambda = i\omega$  into the characteristic function with the real positive angular frequency  $\omega$  and we separate its real and imaginary parts to be zeros. Unfortunately, the boundaries can not be calculated in closed form but by means of numerical methods one can construct stability charts.

Here, we show a case study only, namely, using the parameters of Tab. 1, we analyze the stability of the system. The parameters are based on the laboratory experiments that were carried out in [11]. In order to investigate the stability, we calculated the rightmost characteristic root of the characteristic function against the longitudinal speed  $v$ . The results were also checked by means of the semi-discretization method [20].

The real part and the angular frequency characterizing the rightmost eigenvalue are shown in Fig. 2 for the speed range 10...20 m/s. Panel (a) presents an overview about the location of the rightmost eigenvalue. The vibration frequency is scaled by  $\omega_0 = \sqrt{k_s/m} = 22.36$  rad/s, which refers to the natural angular frequency of the wheel-suspension system without having contact with the ground and without taking into account the mass of tire particles. As it can be observed in panel (b), the vibration frequency is close to  $\omega_0$ . In panel (c), the real part of the eigenvalue is plotted versus the speed. Clearly, these vibrations never decay in time since  $\text{Re} \lambda \geq 0$  in the investigated speed range. Of course, our model does not consider the damping, which can strongly influence these result. This will be the task of future research.

## TIRE DEFORMATIONS

To check the theoretical results and to obtain information about the tire deformations, numerical simulation was carried out. The original IDE-PDEs system Eqns. (11), (3) and (9) were discretized by means of simple finite difference method. The number of spatial mesh points in the contact patch was chosen to 20 while outside the contact patch it was 300. The initial condi-



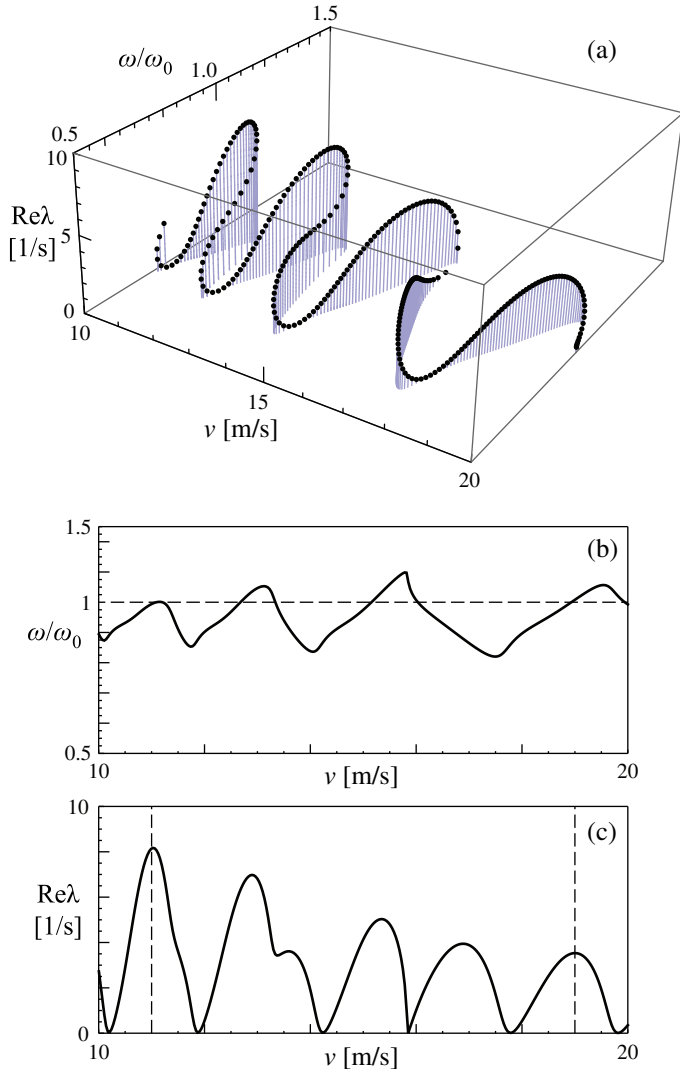


**FIGURE 2.** THE REAL PART OF THE RIGHTMOST EIGENVALUE AND THE CORRESPONDING VIBRATION FREQUENCY OF THE SYSTEM VERSUS THE SPEED.

tions for the numerical simulations were set to zero initial deformation and zero lateral deformation, but non-zero initial lateral speed was applied.

Figure 3 shows the representative tire deformation at two different wheel speeds, which speeds are also marked in Fig. 2c by dashed lines. Obviously, as the wheel speed increases the number of the waves decreases outside the contact patch.

## CONCLUSION

A mechanical model was constructed to investigate the rolling tire attached to a laterally elastic suspension system. The

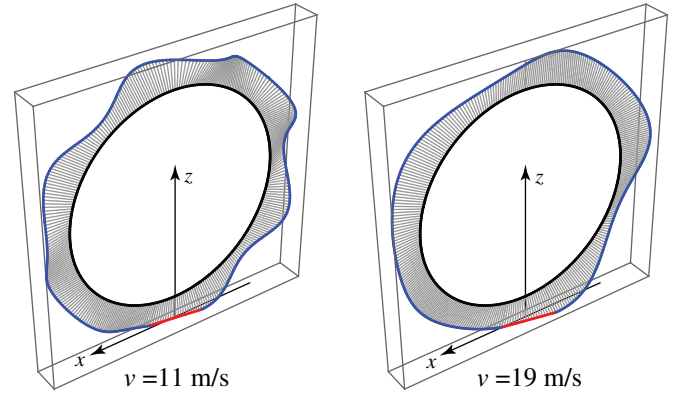


**FIGURE 3.** SIMULATED TIRE DEFORMATIONS AT DIFFERENT SPEEDS.

delayed tire/ground contact model was implemented. Moreover, the lateral tire deformation was also considered outside the contact patch by means of the so-called brush model that also takes into account the mass of the tire particles.

The governing equations of the system were determined and were transformed into the form of neutral delay differential equations. The linear stability analysis of the stationary rolling was analyzed in a case study. It was shown that the interaction of the contact patch and the non-contacting tire particles can lead to tire vibrations in a wide speed range. Although, our model does not consider any source of damping, some of the detected vibrations can be suspected as the origin of noise and heat generation in practice even in the presence of damping.

## ACKNOWLEDGMENT

This research was partly supported by the János Bolyai Research Scholarship of the Hungarian Academy of Sciences and by the Hungarian National Science Foundation under grant no. OTKA PD105442.

## REFERENCES

- [1] Cossalter, V., 2006. *Motorcycle Dynamics*. Lulu Editor.
- [2] Sharp, R. S., Evangelou, S., and Limebeer, D. J. N., 2004. "Advances in the modelling of motorcycle dynamics". *Multibody System Dynamics*, **12**(3), pp. 251–283.
- [3] Besselink, I. J. M., 2000. "Shimmy of aircraft main landing gears". PhD thesis, Technical University of Delft, The Netherlands.
- [4] Terkovic, N., Neild, S., Lowenberg, M., and Krauskopf, B., 2012. "Bifurcation analysis of a coupled nose landing gear-fuselage system". In *Proceedings of AIAA 2012*, AIAA, pp. 1–14. paper No. AIAA 2012-4731.

- [5] Howcroft, C., Krauskopf, B., Lowenberg, M., and Neild, S., 2012. "Effects of freeplay on aircraft main landing gear stability". In Proceedings of AIAA 2012, AIAA, pp. 1–16. paper No. AIAA 2012-4730.
- [6] Brouhiet, G., 1925. "The suspension of the automobile steering mechanism: Shimmy and tramp". *Bull Soc. Ing. Civ. Fr.*, **78**, pp. 540–554.
- [7] Schlippe, B., and Dietrich, R., 1941. "Das Flattern Eines Bepneuten Rades (Shimmying of a pneumatic wheel)". In Bericht 140 der Lilienthal-Gesellschaft für Luftfahrtforschung, pp. 35–45, 63–66. English translation is available in *NACA Technical Memorandum* 1365, pages 125–166, 217–228, 1954.
- [8] Segel, L., 1966. "Force and moment response of pneumatic tires to lateral motion inputs". *Journal of Engineering for Industry, Transactions of the ASME*, **88B**(1), pp. 37–44.
- [9] Pacejka, H. B., 1966. "The wheel shimmy phenomenon". PhD thesis, Technical University of Delft, The Netherlands.
- [10] Stépán, G., 1998. "Delay, nonlinear oscillations and shimmying wheels". In Proceedings of Symposium CHAOS'97, Kluwer Ac. Publ., Dordrecht, pp. 373–386.
- [11] Takács, D., and Stépán, G., 2012. "Micro-shimmy of towed structures in experimentally uncharted unstable parameter domain". *Vehicle System Dynamics*, **50**(11), pp. 1613–1630.
- [12] Takács, D., and Stépán, G., 2013. "Contact patch memory of tyres leading to lateral vibrations of four-wheeled vehicles". *Philosophical Transactions of the Royal Society A: Mathematical, Physical and Engineering Sciences*, **371**(1993).
- [13] Beregi, S., Takacs, D., and Stepan, G., 2015. "Tyre induced vibrations of the car-trailer system". *Journal of Sound and Vibration*. under submission.
- [14] Cesbron, J., Anfosso-Lédée, F., Duhamel, D., Yin, H. P., and Houédec, D. L., 2009. "Experimental study of tyre/road contact forces in rolling conditions for noise prediction". *Journal of Sound and Vibration*, **320**(12), pp. 125 – 144.
- [15] Andersson, P. B. U., and Kropp, W., 2009. "Rapid tyre/road separation: An experimental study of adherence forces and noise generation". *Wear*, **266**(1-2), pp. 129–138.
- [16] O'Boy, D., and Dowling, A., 2009. "Tyre/road interaction noise - Numerical noise prediction of a patterned tyre on a rough road surface". *Journal of Sound and Vibration*, **323**(12), pp. 270 – 291.
- [17] Pinnington, R. J., 2013. "Tyre-road contact using a particle-envelope surface model". *Journal of Sound and Vibration*, **332**(26), pp. 7055 – 7075.
- [18] Hetzler, H., 2009. "On moving continua with contacts and sliding friction: Modeling, general properties and examples". *International Journal of Solids and Structures*, **46**(13), pp. 2556 – 2570.
- [19] Wickert, J. A., and Mote Jr., C. D., 1990. "Classical vibration analysis of axially moving continua". *Journal of Applied Mechanics*, **57**(3), pp. 738–744.
- [20] Insperger, T., and Stépán, G., 2011. *Semi-Discretization for Time-Delay Systems*. Springer, New York.